PERFORMANCE EVALUATION OF KINEMATICALLY REDUNDANT PLANAR PARALLEL MANIPULATORS

João Cavalcanti Santos, Douglas Martins Rocha and Maíra Martins da Silva
University of São Paulo – São Carlos School of Engineering – Departament of Mechanical Engineering
Av. Trabalhador São-carlense, 400, Arnold Schimidt, São Carlos - São Paulo - Brazil - CEP 13566-590
e-mails: joao.cv.santos@gmail.com, douglas.rocha@usp.br, mairams@sc.usp.br

Abstract. *It is known that both actuation and kinematic redundancy promote, among other benefits, a significant reduction in the singularities and homogenization on the actuation forces. However, evaluating if the redundancy is a good solution to increase dynamic performance of a robotic system is not trivial, because this solution means not only that there is more available torque, but also that the inertia of the system has been considerably increased. In this paper, a numerical study is performed to realize whether kinematic redundancy can be a good alternative for planar parallel manipulators to achieve high dynamic performance. Three kinematically redundant configurations of the 3RRR planar manipulator are evaluated through cinematic and dynamic models: the (P)RRR+2RRR, the 2(P)RRR+RRR and the 3(P)RRR. The main objective of this paper is to evaluate numerically the modifications on the workspace and singularity regions due to reconfiguration capabilities caused by this kind of redundancy. Moreover, insights on the trade-off dynamical analysis have been explored. Based on the numerical results, one can conclude that kinematic redundancy has been capable of reducing the maximum required torque to perform a predefined trajectory enhancing the dynamic performance of the manipulator.*

Keywords: *kinematic redundancy, planar manipulators; kinematic and dynamic model; high dynamic performance*

1. INTRODUCTION

For over a decade, parallel kinematic machines (PKM) have attracted the attention of academic and industrial communities due to their advantages over serial architectures. Among these advantages, it can be mentioned the lightness, the high speed/acceleration, the rigidity and the load capacity (Merlet, 1996). The most promising industrial application for these alternative architectures is the pick-and-place operation required in the food, pharmaceutical and electronic industries. Another possible application is the use of haptic PKMs that require high performance, low inertia, high stiffness, low friction, gravitational balancing, multiple degrees of freedom, high compression, among others (Merlet, 1996).

Although providing precision, high stiffness and good dynamic properties, the PKMs suffer from the presence of singularities in their workspace (Conkur and Buckingham, 1997). As a result, the ratio between the useful working space and physical space occupied by the equipment is rather low. Recent results (Kotlarski et al., 2009 and 2011, Mohamed and Gosselin, 2005) have suggested that the use of redundancy can be a good alternative for minimizing the presence of singularities. For PKMs, the concept of redundancy can be classified into (Merlet, 1996):

- Sensor redundancy which occurs when the number of sensors is higher that the number of degrees-of-freedom. This methodology is mainly used for calibration of robotic systems or control purposes.
- Actuation redundancy happens when there is the introduction of a kinematic chain in the mechanism.
- Kinematic redundancy corresponds to the introduction of an actuator in a kinematic chain. Due to the kinematic redundancy, the mechanism can reconfigure itself to avoid the singularities as explored by Kotlarski et al. (2009).

In order to illustrate the differences between actuation and kinematic redundancies, Fig. 1 depicts the planar parallel manipulator 3RRR, the redundantly actuated planar parallel manipulators 4RRR and the kinematically redundant planar parallel manipulator (P)RRR+2RRR, where R and P stand for revolute and prismatic joints, respectively. The underline letters indicate the joints that are actuated and the letter between parentheses indicated the redundancy.

The aim of this work is to study whether the kinematic redundancy can be a good alternative for parallel planar manipulators to achieve high accelerations. Mohamed and Gosselin (2005) affirmed that redundancy can, in general, improve the ability and performance of parallel manipulators. According to these authors, using the extra degrees of freedom, the redundant mechanism will not only execute the original output task but also additional tasks such as eliminating singularities, increasing the workspace, improving dexterity and obstacle avoidance, optimizing force transmission, and/or compensating for unexpected impact. The main reason behind these benefits is that a predefining task can be performed in several manners; therefore a cost function can be defined to treat all the conflicting objectives in an interesting fashion. The use of actuation redundancy in planar manipulators has been recently studied by Rocha and da Silva (2013). In this work, it has been concluded that actuation redundancy have been capable of enlarging the usable workspace since the singularity region has been considerably reduced and that in spite of having more available torque, the added inertia limited the dynamic performance of the redundant manipulators.

In this way, regarding conflicting objectives, evaluating if the kinematic redundancy is a good solution to increase dynamic performance of a robotic system is not trivial, because this solution means not only that there is more torque available, but also that the inertia of the system has been considerably increased. In order to infer about this quest, kinematic and dynamic models of different configurations of a planar parallel manipulator are developed. Based on these models, workspace and singularity analyses are carried out. The studied configurations are the planar parallel manipulator 3RRR and the kinematically redundant planar parallel manipulators (P)RRR+2RRR, 2(P)RRR+RRR and 3(P)RRR, shown in Fig. 2.

The proposed setup is composed of 3 linear motors (the redundant actuators) and 3 rotational motors. If the linear motors are going to be actuated or not define the redundancy of the system, as illustrated in Fig. 2. For instance, if only one linear motor can be actuated, the system has an extra degree-of-freedom yielding to the (P)RRR+2RRR configuration.

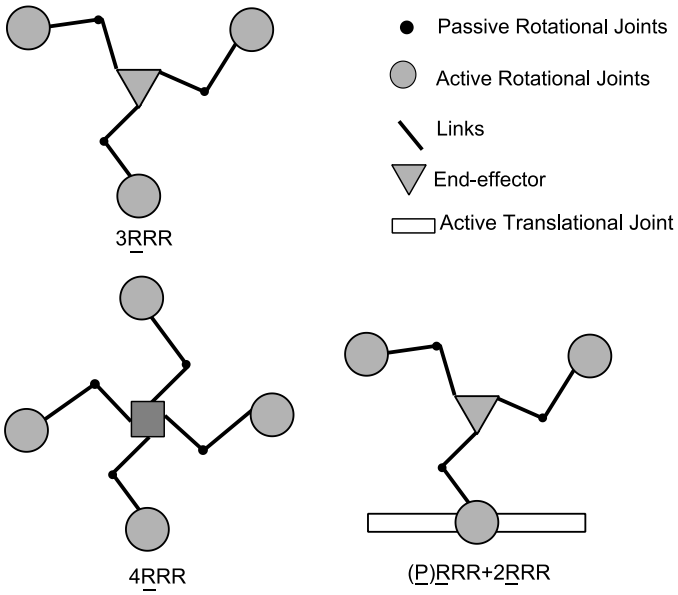

Figure 1. 3RRR: planar parallel manipulator, 4RRR: redundant actuated planar manipulator and (P)RRR+2RRR: planar kinematically redundant planar manipulator

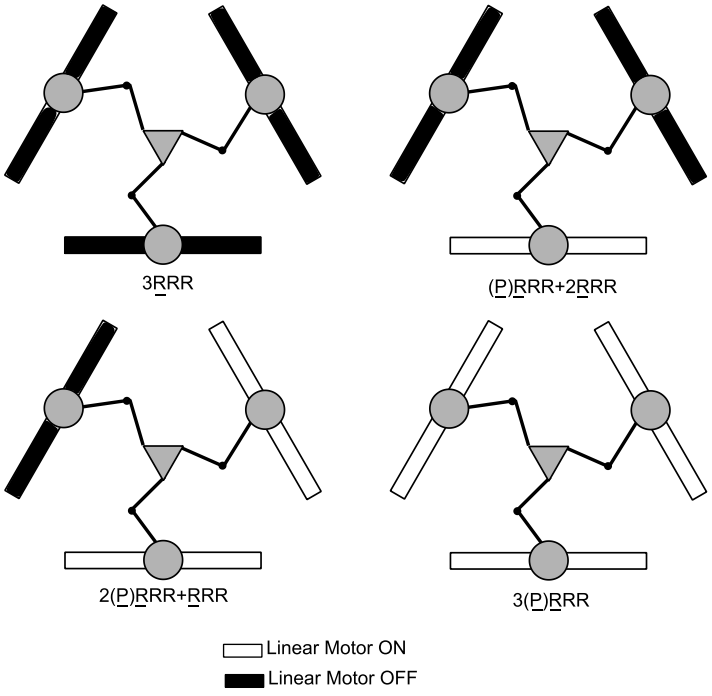

Figure 2. 3RRR: planar parallel manipulator, (P)RRR+2RRR: one redundant actuator, 2(P)RRR+RRR: two redundant actuators and 3RRR: three redundant actuators

The redundant actuator can be considered generally in two manners: the offline and the online (Kotlarski et al.,2011). The offline manner is the simplest way to use the redundant actuator since its position is modified before the performance of the desired trajectory. This position is selected according to singularity avoidance and performance indexes. According to Kotlarski et al. (2011), this approach leads to satisfactory results in the case of repeated and simple trajectories. The online manner exploits the full capacity of the redundant actuators updating their position while the trajectory is being performed. This strategy requires a dynamic optimization strategy which may lead to very efficient alternatives to perform the desired strategies. Nevertheless, this strategy demands higher computational effort.

In this manuscript, the offline strategy is adopted. In order words, a search for the most adequate positions for the linear redundant actuators is carried out before the performance of the desired trajectory. A consequence of this choice is that the redundant configurations can be evaluated by using the 3RRR kinematic and dynamic models by modifying the position of the linear redundant actuators.

The numerical methodology employed to model the 3RRR manipulator is described in Section 2. The numerical results regarding the modifications on the workspace and singularity regions regarding the addition of the redundant actuator are treated in Section 3. Also in Section 3, a desired trajectory is selected and the required torque to perform it is calculated by the non-redundant and redundant manipulators. Finally, in Section 5, conclusions are drawn.

2. NUMERICAL ANALYSES

Numerical analyses have been carried out using the inverse kinematic and dynamic models of the 3RRR in order to evaluate the different configurations regarding cinematic, dynamic, workspace and singularity analysis. Theoretical aspects are treated hereafter. Figure 3 illustrates the parameters used to evaluate the 3RRR numerical model. As it can be seen, the mechanism is composed by 3 kinematic chains (links) containing 1 active rotational joint (motor) and 2 passive joints. A similar methodology has been employed by Rocha and da Silva (2013).

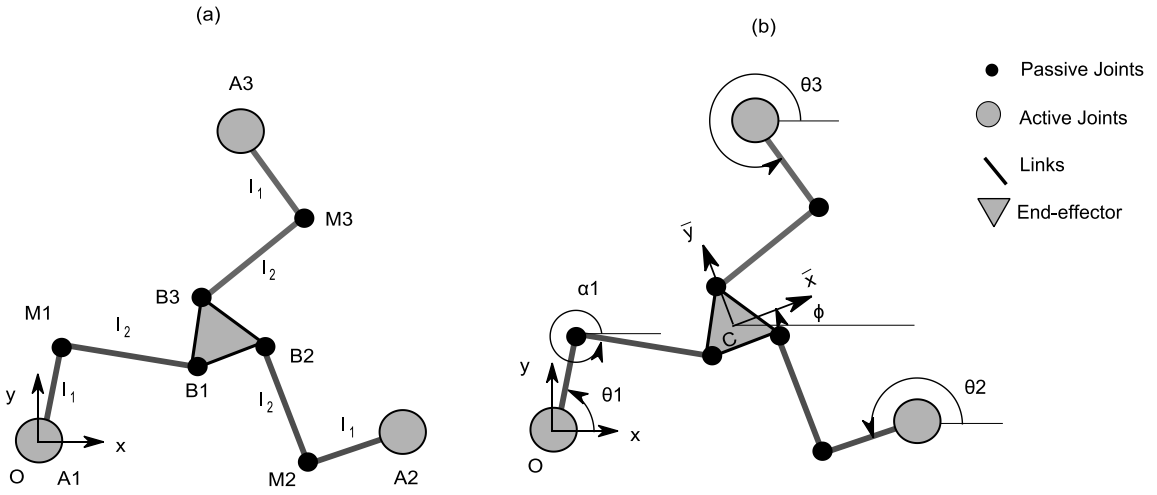

Figure 3. 3RRR geometrical characteristics: (a) length of the links and (b) joint angles

2.1 Cinematic Analysis

As suggested by Wu *et al.* (2011), the base coordinate system O-xy is fixed on the active revolute joint A1 and the moving coordinate system C-$\overline{xy}$ is connected at the center of the end-effector (see Fig. 2). The inverse kinematic models of the 3RRR manipulator can be solved by evaluating the positions of the passive joints and the end-effector. This can be performed by describing the position of the passive joints by M_i through the variables θ_i and the known positions $_i$ and B_i. In this way, the vector M_iB_i, which has a fixed length l_2^i, can be found by knowing that $_iB_i = -OA_i + OC + R_\phi CB_i$ and $A_iM_i = R_\theta L_1^i$:

$$M_iB_i = \ _iB_i - A_iM_i = -OA_i + OC + R_\phi CB_i - R_\theta L_1^i \tag{1}$$

where R_ϕ and R_θ are rotation matrices and L_1^i is a vector described by:

$$R_\phi = \begin{bmatrix} \cos\phi & -\sin\phi \\ \sin\phi & \cos\phi \end{bmatrix}, \qquad R_\theta = \begin{bmatrix} \cos\theta_i & -\sin\theta_i \\ \sin\theta_i & \cos\theta_i \end{bmatrix}, \qquad L_1^i = \begin{bmatrix} l_1^i \\ 0 \end{bmatrix} \tag{2}$$

According to Fig. 2, Eq. (2) can be rewritten as:

$$M_iB_i = -\begin{bmatrix} x_{Ai} \\ y_{Ai} \end{bmatrix} + \begin{bmatrix} x_C \\ y_C \end{bmatrix} + \begin{bmatrix} \cos\phi & -\sin\phi \\ \sin\phi & \cos\phi \end{bmatrix} \begin{bmatrix} \bar{x}_{CBi} \\ \bar{y}_{CBi} \end{bmatrix} - \begin{bmatrix} \cos\theta_i & -\sin\theta_i \\ \sin\theta_i & \cos\theta_i \end{bmatrix} \begin{bmatrix} l_1^i \\ 0 \end{bmatrix} \tag{3}$$

Using the relation $|M_iB_i|^2 = (l_2^i)^2$, Eq. (3) can be described by the following set of equations:

$$E1_i \sin\theta_i + E2_i \cos\theta_i + E3_i = 0 \tag{4}$$

where

$$\begin{cases} E1_i = Kx_i{}^2 + Ky_i{}^2 - T_i + 1 \\ E2_i = -2Kx_i \\ E3_i = -2Ky_i \end{cases} \tag{5}$$

and

$$\begin{cases} Kx_i = \frac{(x - x_{Ai} + \bar{x}_{CBi}\cos\phi - \bar{y}_{CBi}\sin\phi)}{l_1^i} \\ Ky_i = \frac{(y - y_{Ai} + \bar{x}_{CBi}\sin\phi + \bar{y}_{CBi}\cos\phi)}{l_1^i} \\ T_i = \frac{(l_2^i)^2}{(l_1^i)^2} \end{cases} \tag{6}$$

It can be observed that Eq. (4) depends only on the following variables x, y, ϕ and the mechanism dimensions. Equation 4 can be solved by using the Weierstress substitution (Mabie and Reinholtz, 1987):

$$\cos\theta_i = \frac{1-\lambda^2}{1+\lambda^2}\ ,\ \sin\theta_i = \frac{2\lambda}{1+\lambda^2}\ ,\ \tan\frac{\theta_i}{2} = \lambda \tag{7}$$

Substituting Eqs. (7) into Eq. (4), the angles θ_i can be calculated:

$$\theta_i = 2\tan^{-1}\left(\frac{-E1_i \pm \sqrt{E1_i{}^2 + E2_i{}^2 - E3_i{}^2}}{E3_i - E2_i}\right) \tag{8}$$

Based on the angles θ_i, one can calcutate the angles α_i (see Fig. 3) through the vector M_iB_i given by Eq. (3):

$$\alpha_i = \tan^{-1}\left(\frac{y_{MiBi}}{x_{MiBi}}\right) \tag{9}$$

According to Eq. (8), each angle θ_i can assume two different values. In this way, there are several possible combinations of considering these different values. Therefore, considering all possibilities for the 3RRR planar manipulator, a single end-effector position (x_C, y_C and ϕ) can be obtained by 8 distinct combinations of the angles θ_i.

In order to evaluate the velocities and the accelerations of the passive and active joints of the manipulators, one can express the end-effector position using the following equation:

$$OC = \begin{bmatrix} x_C \\ y_C \end{bmatrix} = \begin{bmatrix} x_{Ai} \\ y_{Ai} \end{bmatrix} + \begin{bmatrix} \cos\theta_i & -\sin\theta_i \\ \sin\theta_i & \cos\theta_i \end{bmatrix} \begin{bmatrix} l_1^i \\ 0 \end{bmatrix} - \begin{bmatrix} \cos\phi & -\sin\phi \\ \sin\phi & \cos\phi \end{bmatrix} \begin{bmatrix} \bar{x}_{CBi} \\ \bar{y}_{CBi} \end{bmatrix} + \begin{bmatrix} \cos\alpha_i & -\sin\alpha_i \\ \sin\alpha_i & \cos\alpha_i \end{bmatrix} \begin{bmatrix} l_2^i \\ 0 \end{bmatrix} \tag{10}$$

It is useful to the define the terms Fx_i and Fy_i in the following way

$$\begin{bmatrix} x_C \\ y_C \end{bmatrix} = \begin{bmatrix} x_{Ai} + l_1^i\cos\theta_i - \cos\phi\,\bar{x}_{CBi} + \bar{y}_{CBi}\sin\phi + l_2^i\cos\alpha_i \\ y_{Ai} + l_1^i\sin\theta_i\ - \bar{x}_{CBi}\sin\phi - \bar{y}_{CBi}\cos\phi + l_2^i\sin\alpha_i \end{bmatrix} = \begin{bmatrix} Fx_i \\ Fy_i \end{bmatrix} \tag{11}$$

Equation 11 can be rewritten considering all the mechanism legs:

$$\begin{bmatrix} x_C \\ y_C \end{bmatrix} = \frac{1}{3}\begin{bmatrix} Fx_1 + Fx_2 + Fx_3 \\ Fy_1 + Fy_2 + Fy_3 \end{bmatrix}_{3RRR} \tag{12}$$

Taking the time derivative of Eq. (12) and rearranging the terms, one can yield the following expression:

$$\dot{p} = \begin{bmatrix} \dot{x}_C \\ \dot{y}_C \\ \dot{\phi} \end{bmatrix} = J_{pq}[\dot{\theta}_1 \quad \dot{\theta}_2 \quad \dot{\theta}_3 \quad \dot{\alpha}_1 \quad \dot{\alpha}_2 \quad \dot{\alpha}_3 \quad \dot{\phi}]^T = J_{pq}\dot{q} \tag{13}$$

The matrix J_{pq} is known as Jacobian and can be non-squared. Therefore, in order to obtain the relation for $\dot{q}$ from $\dot{p}$, the pseudo inverse matrix J'_{pq} should be calculated and employed in the following relation:

$$\left(J_{pq}{}^{T} J_{pq}\right)^{-1} J_{pq}{}^{T} \dot{p} = J'_{pq} \dot{p} = \dot{q} \tag{14}$$

The accelerations can be easily calculated by time deriving Eq. (13), yielding:

$$\ddot{q} = J'_{pq} \ddot{p} + \dot{J}'_{pq} \dot{p} \tag{15}$$

2.2 Dynamic Analysis

The inverse dynamic model consists in obtaining the required torques and forces to move the manipulator according to a predefined trajectory. Some important issues should be considering when dynamic modeling PKMs. A major issue is related to singular points in the workspace (Siciliano and Khatib, 2008). This issue is treated in the following sections. One can use different methodologies to formulate the dynamic model. Among them, we would like to highlight the Principle of Virtual Work and the Lagrange Formulation (Merlet, 1996). Considering the later methodology, the general equation of motion of a PKM can be described by (Siciliano and Khatib, 2008):

$$M\ddot{q} + C\dot{q} + \tau_g = \tau + \tau_a + \tau_c \tag{18}$$

where $\ddot{q}$, $\dot{q}$ and q are the acceleration, velocity and position vectors, respectively, M and C are the inertia and the Coriolis related matrices, and τ, τ_g, τ_a and τ_c are the force vectors related to the actuators forces, gravitational force, spring and damping forces and joint forces (associated to the closed kinematic chain), respectively. For a planar manipulator, τ_g and τ_a can be considered null. One strategy to solve Eq. (18) is to rewrite this equation considering the constraints' equations ($\eta(\theta) = 0$). Taking the time derivatives of the equation of constraints, one can obtain the Jacobian matrix $J_{\eta q}$:

$$\dot{\eta} = J_{\eta q} \dot{q} = 0 \tag{19}$$
$$\ddot{\eta} = J_{\eta q} \ddot{q} + \dot{J}_{\eta q} \dot{q} \tag{20}$$

where $J_{\eta q} = \partial \eta / \partial q$. The forces related to the joints can be expressed in terms of the Lagrange multipliers λ (Rao, 2009), according to Eq. (21):

$$\tau_c = J_{\eta q}{}^{T} \lambda \tag{21}$$

In this manner, Eq. (18) can be rewritten in the following way:

$$M\ddot{q} + C\dot{q} = \tau + J_{\eta q}{}^{T} \tag{22}$$

The most straightforward way to solve this equation is to rewrite it considering the Jacobian matrix $J_{q\theta}$, which correlates the time derivatives of the generalized coordinates and the actuators' angular positions ($\dot{q} = J_{q\theta}\dot{\theta}$ and $\ddot{q} = J_{q\theta}\ddot{\theta} + \dot{J}_{q\theta}\dot{\theta}$):

$$MJ_{q\theta}\ddot{\theta} + \left(M\dot{J}_{q\theta} + CJ_{q\theta}\right)\dot{\theta} = \tau + J_{\eta q}{}^{T} \lambda \tag{23}$$

Pre-multiplying Eq. (23) by $J_{q\theta}{}^{T}$, one gets the following expression:

$$J_{q\theta}{}^{T} M J_{q\theta} \ddot{\theta} + J_{q\theta}{}^{T}\left(M\dot{J}_{q\theta} + CJ_{q\theta}\right)\dot{\theta} = J_{q\theta}{}^{T}\tau + J_{q\theta}{}^{T} J_{\eta q}{}^{T} \lambda \tag{24}$$

From Eqs. (19) and $\dot{q} = J_{q\theta}\dot{\theta}$, one can infer that $J_{\eta q}\dot{q} = J_{\eta q} J_{q\theta}\dot{\theta} = 0$, where $\dot{\theta}$ can assume any value. In this way, it can be concluded that $J_{\eta\theta} J_{q\theta} = 0$ and $J_{\eta\theta}{}^{T} J_{q\theta}{}^{T} = 0$. Defining $J_{q\theta}{}^{T} M J_{q\theta} = M_\theta$, $J_{q\theta}{}^{T}\left(M\dot{J}_{q\theta} + CJ_{q\theta}\right) = C_\theta$ and $\tau_\theta = J_{q\theta}{}^{T}\tau$, it is possible to express the actuators' torques τ_θ in terms of $\ddot{\theta}, \dot{\theta}$ e θ:

$$M_\theta \ddot{\theta} + C_\theta \dot{\theta} = \tau_\theta \tag{25}$$

It is important to highlight that Eq. (25) is only valid when the relation $\dot{q} = J_{q\theta}\dot{\theta}$ is clearly defined, *i.e.*, the manipulator is not on a singularity position. Singularity analysis is treated hereafter.

Considering the 3RRR manipulator the constraints' equations ($\eta(\theta) = 0$) can be determined observing the closed-loop connections A_1A_2 and A_3A_2 (see Fig. 3). From these closed-loop connections, four equations of constraints can be derives:

$$\eta_1 = x_{A1} + l_1^1 \cos\theta_1 + l_2^1 \cos\alpha_1 + L_{CG1}\cos(\phi + \beta_1) + L_{CG2}\cos(\phi + \beta_2) - l_2^2 \cos\alpha_2 - l_1^2 \cos\theta_2 - x_{A2} = 0 \quad (26)$$

$$\eta_2 = y_{A1} + l_1^1 \sin\theta_1 + l_2^1 \sin\alpha_1 + L_{CG1}\sin(\phi + \beta_1) + L_{CG2}\sin(\phi + \beta_2) - l_2^2 \sin\alpha_2 - l_1^2 \sin\theta_2 - y_{A2} = 0 \quad (27)$$

$$\eta_3 = x_{A3} + l_1^3 \cos\theta_3 + l_2^3 \cos\alpha_3 + L_{CG3}\cos(\phi + 3) + L_{CG2}\cos(\phi + \beta_2) - l_2^2 \cos\alpha_2 - l_1^2 \cos\theta_2 - x_{A2} = 0 \quad (28)$$

$$\eta_4 = y_{A3} + l_1^3 \sin\theta_3 + l_2^3 \sin\alpha_3 + L_{CG3}\sin(\phi + \beta_3) + L_{CG2}\sin(\phi + \beta_2) - l_2^2 \sin\alpha_2 - l_1^2 \sin\theta_2 - y_{A2} = 0 \quad (29)$$

where β_i is the angle the vector B_iC and the horizontal line and $L_{CGi} = |B_iC|$. Taking the time derivative of these equations, one gets:

$$\frac{\partial\eta}{\partial\theta}\dot{\theta} + \frac{\partial\eta}{\partial\psi}\dot{\psi} = 0 \quad (30)$$

where $\theta = [\theta_1 \quad \theta_2 \quad \theta_3]^T$ and $\psi = [\alpha_1 \quad \alpha_2 \quad \alpha_3 \quad \phi]^T$. Through this relation, it is possible to define the Jacobian matrix $J_{\psi\theta}$:

$$\dot{\psi} = -\frac{\partial\eta}{\partial\psi}^{-1}\frac{\partial\eta}{\partial\theta}\dot{\theta} = J_{\psi\theta}\dot{\theta}, \det\left(\frac{\partial\eta}{\partial\psi}\right) \neq 0 \quad (31)$$

Equation 30 correlates the velocity of the passive and active joints and the Jacobian matrix $J_{\psi\theta}$can be used to calculate the Jacobian matrix $J_{q\theta}$:

$$\dot{q} = \begin{bmatrix} I_3 \\ J_{\psi\theta} \end{bmatrix}\dot{\theta} = J_{q\theta}\dot{\theta} \quad (32)$$

2.3 Singularity Analysis

Singularity regions are characterized by an important lack of stiffness. The analysis of these regions can be performed by evaluating the rank of Jacobian matrix that correlates the output velocities $\dot{p}$ with the actuators velocities $\dot{\theta}$ (Bonev and Gosselin, 2001):

$$J_p\dot{p} = J_\theta\dot{\theta} \quad (32)$$

As described by Gosselin and Angeles (1990), there are three different types of singularities regarding PKM:

1. The first type of singularity is when $\det(J_\theta) = 0$. This kind of singularity is similar to the ones that usually happen in a serial manipulator. It occurs at the workspace boundaries when the legs of the mechanism are collinear.
2. The second type of singularity is when $\det(J_p) = 0$. In this situation, the end-effector can move even when the actuators are not acting. In the case of PKMs, this kind of singularity happens when the rank of the Jacobian matrix J_p is smaller than the system degrees of freedom. This can be also calculated by $\det(J_p{J_p}^T) = 0$.
3. The third type of singularity happens when J_θ and J_p are singular simultaneously.

In order to evaluate the singularity regions of the PKMs, the matrices J_p and J_θ should be calculated. According to Bonev and Gosselin (2001), this can be done by calculating the amplitude of the vector that describes the link l_2^i of the manipulator:

$$(l_2^i)^2 = \left(-OA_i + OC + R_\phi CB_i - R_\theta L_1^i\right)^T\left(-OA_i + OC + R_\phi CB_i - R_\theta L_1^i\right) \quad (33)$$

Taking the time derivative of Eq. (33) and recalling Eq. (3), one can obtain:

$$M_i{B_i}^T\left(\begin{bmatrix}\dot{x}_C \\ \dot{y}_C\end{bmatrix} + E_\phi R_\phi CB_i\dot{\phi} - l_1^i\dot{\theta}_i R_{\theta i}E_\theta\right) = 0 \quad (34)$$

where $E_\phi = \begin{bmatrix}0 & -1 \\ 1 & 0\end{bmatrix}$ and $E_\theta = \begin{bmatrix}0 \\ 1\end{bmatrix}$. Rewritting Eq. (33), one can obtain the matrices J_p and J_θ for the 3RRR:

$$\underbrace{\begin{bmatrix} M_1{B_1}^T,\ M_1{B_1}^T E_\phi R_\phi C B_1 \\ \vdots \\ M_k{B_k}^T,\ M_k{B_k}^T E_\phi R_\phi C B_k \end{bmatrix}}_{J_p} \begin{bmatrix} \dot{x}_C \\ \dot{y}_C \\ \dot{\phi} \end{bmatrix} = \underbrace{\begin{bmatrix} M_1{B_1}^T(-l_1^i)R_{\theta 1}E_\theta & 0 & \cdots & 0 \\ 0 & M_2{B_2}^T(-l_1^i)R_{\theta 2}E_\theta & \cdots & 0 \\ \vdots & \vdots & \ddots & \vdots \\ 0 & 0 & \cdots & M_k{B_k}^T(-l_1^i)R_{\theta k}E_\theta \end{bmatrix}}_{J_\theta} \begin{bmatrix} \dot{\theta}_1 \\ \dot{\theta}_2 \\ \vdots \\ \dot{\theta}_k \end{bmatrix} \tag{35}$$

The singularity points can be obtained by discretizing the workspace in Q points and verifying the rank of the matrices J_p and J_θ.

2.4 Workspace Analysis

The workspace area is estimated by the intersection of the ring-shape areas that each leg *i* can reach according to the maximum and minimum lengths that this can leg can reach, which can be calculated according to Eqs. (36) and (37):

$$|A_iB_i|_{máx} = l_1^i + l_2^i \tag{36}$$

$$|A_iB_i|_{mín} = \begin{cases} l_1^i - l_2^i,\ se\ l_1^i - l_2^i > 0 \\ 0,\ se\ l_1^i - l_2^i \le 0 \end{cases} \tag{37}$$

In this way, the maximum and minimum lengths that the leg *i* can reach considering a fixed end-effector orientation, $t \in [0,2\pi]$,.can be calculated by:

$$OC_{i-máx}^{fixed} = \begin{bmatrix} x_{Ai} \\ y_{Ai} \end{bmatrix} + \begin{bmatrix} |A_iB_i|_{máx}\cos t \\ |A_iB_i|_{máx}\sin t \end{bmatrix} - R_\phi C B_i = \begin{bmatrix} |A_iB_i|_{máx}\cos t - \bar{x}_{CBi}\cos\phi + \bar{y}_{CBi}\sin\phi \\ |A_iB_i|_{máx}\sin t - \bar{x}_{CBi}\sin\phi - \bar{y}_{CBi}\cos\phi \end{bmatrix} \tag{38}$$

$$OC_{i-mín}^{fixed} = \begin{bmatrix} x_{Ai} \\ y_{Ai} \end{bmatrix} + \begin{bmatrix} |A_iB_i|_{mín}\cos t \\ |A_iB_i|_{mín}\sin t \end{bmatrix} - R_\phi C B_i = \begin{bmatrix} |A_iB_i|_{mín}\cos t - \bar{x}_{CBi}\cos\phi + \bar{y}_{CBi}\sin\phi \\ |A_iB_i|_{mín}\sin t - \bar{x}_{CBi}\sin\phi - \bar{y}_{CBi}\cos\phi \end{bmatrix} \tag{39}$$

The total workspace considering a variable end-effector orientation can be given by the intersection of the ring-shape areas that each leg *i* and the end-effector can reach. Therefore, the maximum and minimum ring-shape radiuses for a variable end-effector orientation can be found by:

$$OC_{i-máx}^{total} = \begin{bmatrix} |A_iC|_{máx}\cos t \\ |A_iC|_{máx}\sin t \end{bmatrix} \tag{40}$$

$$OC_{i-mín}^{total} = \begin{bmatrix} |A_iC|_{mín}\cos t \\ |A_iC|_{mín}\sin t \end{bmatrix} \tag{41}$$

3. NUMERICAL RESULTS

A pre-defined straight line trajectory within the total workspace area has been selected to evaluate the three different configurations. Figure 4 depicts the position, velocity and acceleration profile of this pre-defined trajectory. As can be seen in Fig. 4, the manipulator performing the pre-defined trajectory starts and finish the motion with null velocity reaching a maximum acceleration of 4 m/s² and angular acceleration of 5.2 rad/s². For sake of illustration Fig. 5 shows the initial and the final position of the end-effector for the desired trajectory.

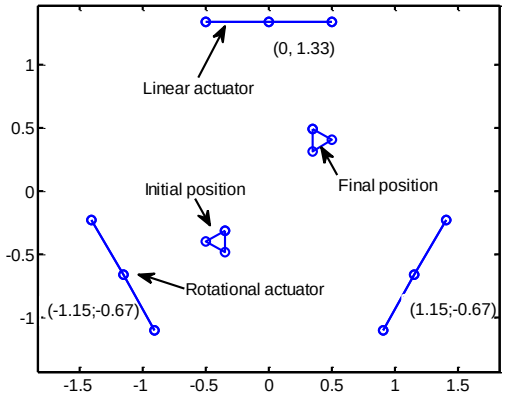

Figure 4. Pre-defined trajectory: initial and final end-effector position

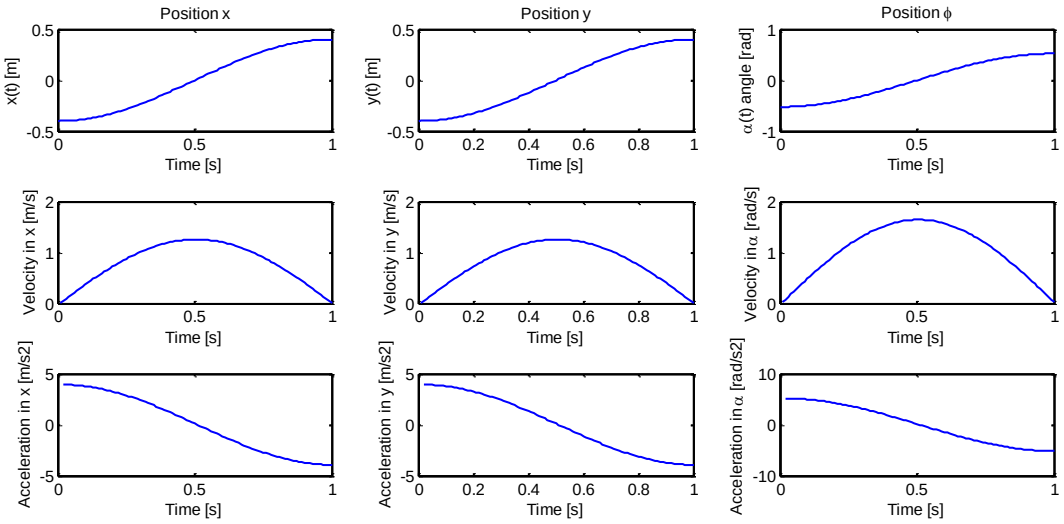

Figure 5. Pre-defined trajectory: position, velocity and acceleration of the end-effector

The nominal positions of the rotational actuators are also shown in Fig. 4 (A1, A2 and A3 in Fig. 3a). Their nominal positions are described in Table 1. The stroke of translational actuators is 1m and their arrangements are illustrated in Figs. 4, 5 and 6. The length of each link is l_1 and l_2 is also 1m. Each rotational actuator weights 0.4kg as well the links.

Table 1. Rotational Actuators' Positions.

Rotational Actuators	x	y
A1	0.00	1.33
A2	1.15	-0.67
A3	-1.15	-0.67

3.1 Workspace and Singularity Regions

Based on the methodology described in Section 2, the workspace and the singularity regions for the non-redundant and the redundant manipulators have been calculated. Figure 6 shows these regions for the non-redundant manipulator, the 3RRR, considering a constant $\phi = 0$. In Figs. 6 and 7, the linear actuators are represented by a line and the rotational actuators are represented by a circle.

In order to illustrate the reconfiguration capabilities of the redundant manipulators, the workspace and singularity regions of different configurations are depicted in Fig. 7. In this figure, the position of one rotational actuator has been modified by the linear actuator before the actual robot movement to perform a desired trajectory. As it can be seen, the understudied regions are adapted when the position of one rotational actuator is modified. In this way, one can decide the best configuration for a pre-determined movement. This selection can be done in order to avoid singularities and regions out of the workspace.

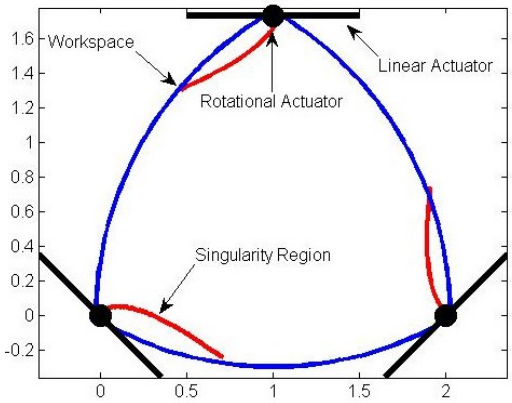

Figure 6. Workspace and singularity regions for the non-redundant manipulator 3RRR

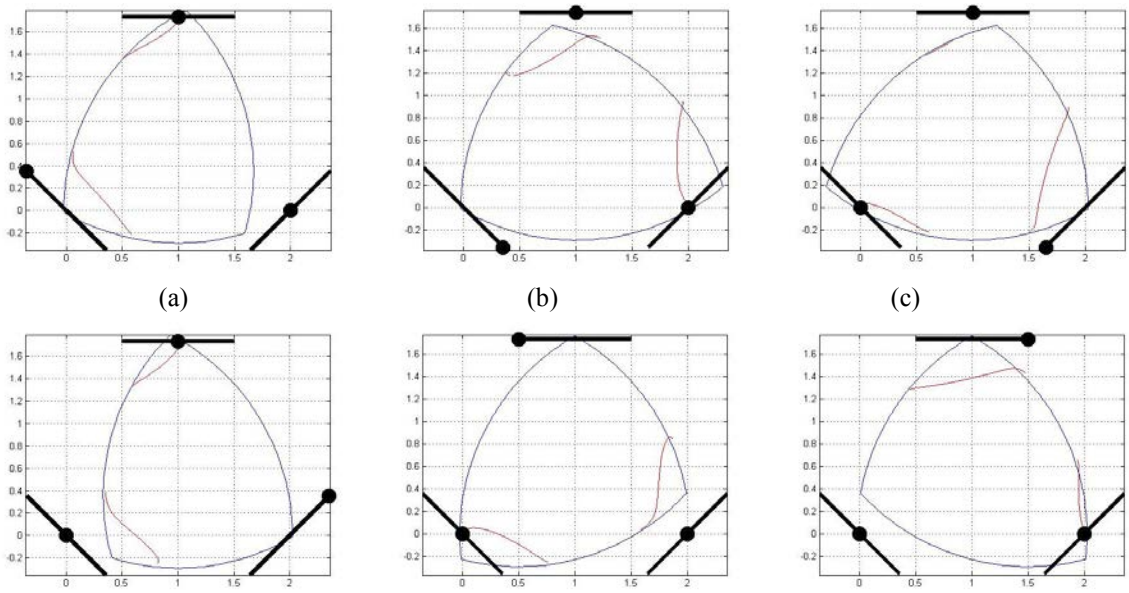

(a) (b) (c)

(d) (e) (f)

Figure 7. Workspace and singularity regions for the redundant manipulators

3.2 Dynamic Analisys

In order to evaluate the system dynamically, the required torque to perform a pre-defined trajectory (see Fig. 5) has been evaluated using the methodology described in Section 2. Figure 8a shows the required torque to perform the pre-defined trajectory by the non-redundant manipulator, the 3RRR illustrated in Fig. 9a. The maximum required torque is 10.55N.m.

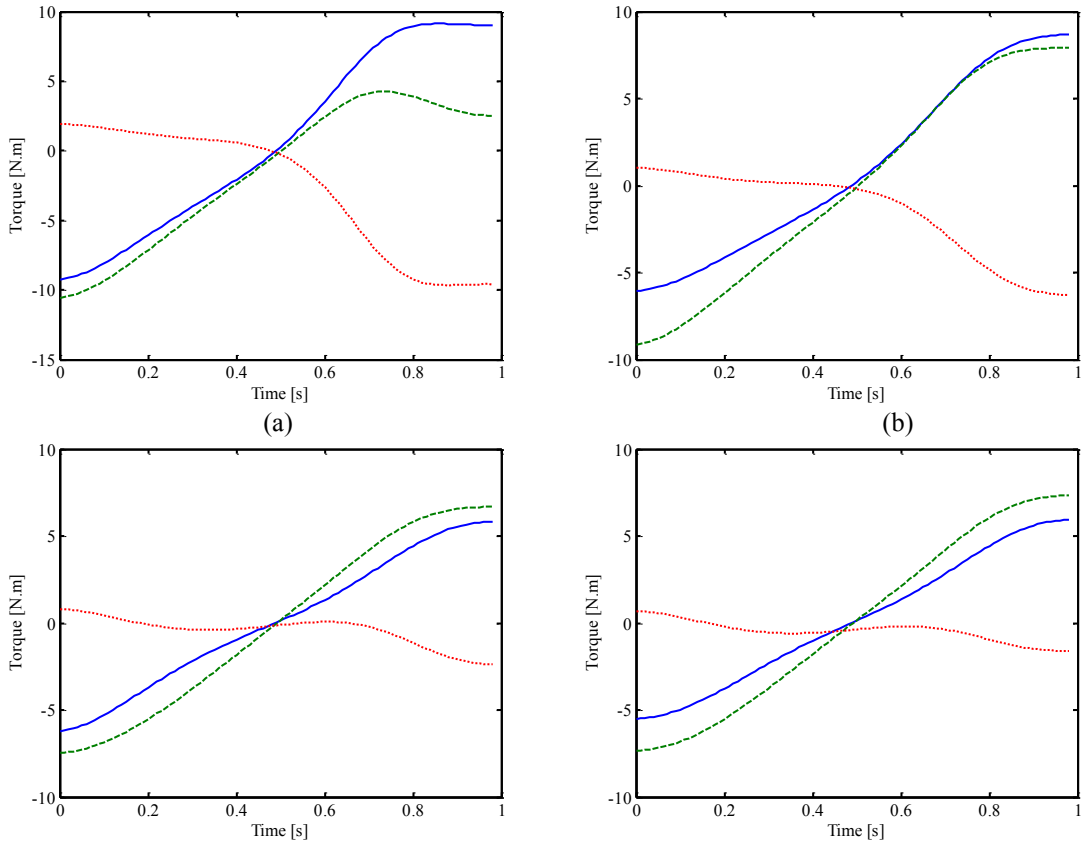

Figure 8. Required torque for the best configuration of the (a) 3RRR, (b) (P)RRR+2RRR, (c) 2(P)RRR+RRR and (d) 3(P)RRR+2RRR

The maximum required torque is an important metric for the design of robotic system, since based on this value, the motors can be selected. In this way, in order to evaluate the impact of the redundancy on the robot system dynamics, the maximum torque value is going to be evaluated for each redundant manipulator. Each linear actuator stroke has been subdivided in 10 equidistant positions, from -0.5 to 0.5, and the maximum torque has been extensively evaluated. Firstly, the (P)RRR+2RRR has been evaluated. This configuration has only one redundant linear actuator (actuator A1 from Table 1) and 10 different configurations have been investigated. Modifying the position of this linear actuator to +0.4 as illustrated in Figure 9b guarantees a maximum required toque of 9.13N.m. Figure 8b shows the required torque to perform the pre-defined trajectory for this redundant manipulator.

The same strategy has been employed for the non-redundant manipulators 2(P)RRR+RRR and 3(P)RRR. They have two and three redundant linear actuators (actuator A2 and A3 from Table 1), respectively. The evaluation of the 2(P)RRR+RRR required the calculation of 100 possibilities while the evaluation of the 3(P)RRR, 1000 possibilities. The best options are described in Table 2 and illustrated in Fig. 9. For the 2(P)RRR+RRR and 3(P)RRR, the maximum required torques have been reduced to 7.47N.m and 7.33N.m, respectively.

Table 2. The optimal configuration for each redundant manipulator and the maximum required torque

Manipulator	Number of redundant actuators	A1	A2	A3	Maximum required torque (N.m)
3RRR	0	0	0	0	10.55
(P)RRR+2RRR	1	0.4	0	0	9.13
2(P)RRR+RRR	2	0.3	-0.5	0	7.47
3(P)RRR	3	0.3	-0.5	-0.5	7.33

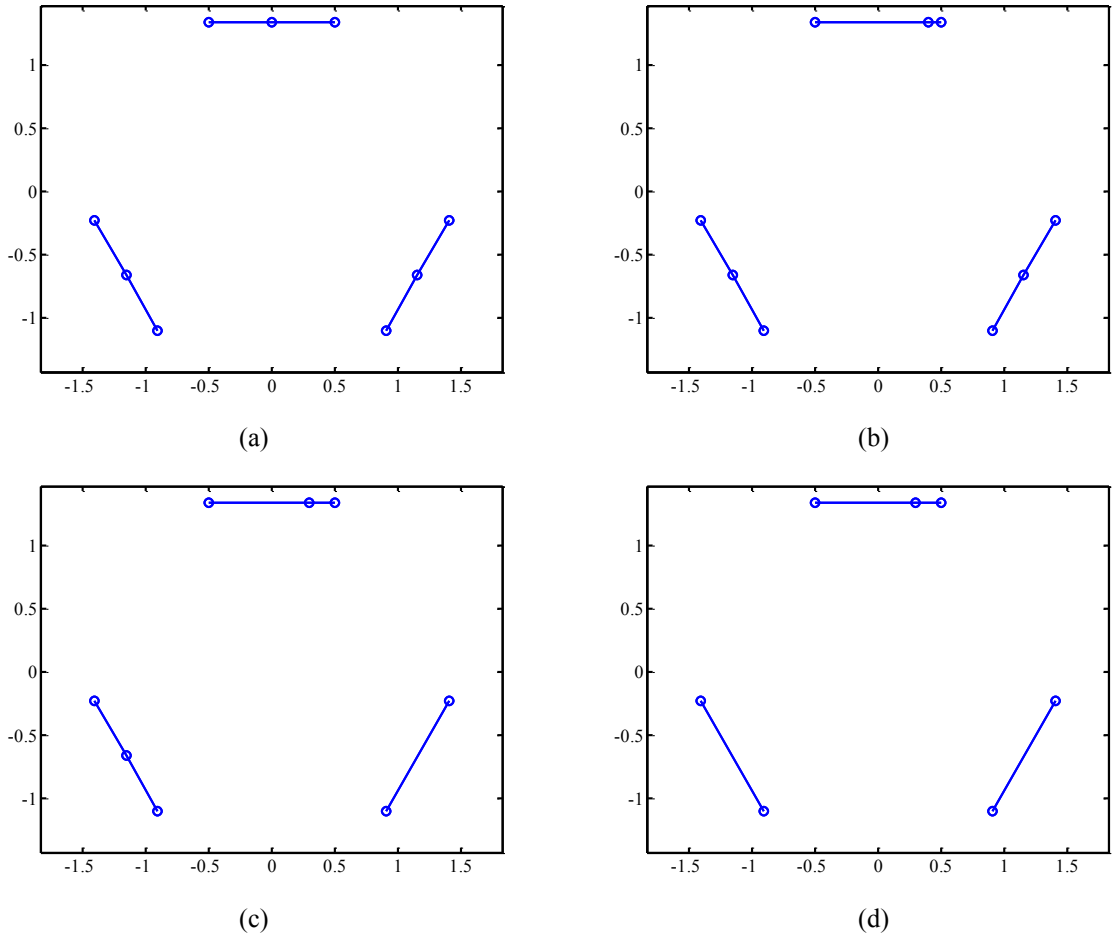

Figure 9. The best configuration of the (a) 3RRR, (b) (P)RRR+2RRR, (c) 2(P)RRR+RRR and (d) 3(P)RRR+2RRR

4. CONCLUSIONS

Based on the numerical results, one can conclude that kinematically redundant manipulators have been capable of adapting to perform a desired task. This adaptation can be performed online, by the actuation of the redundant motor during the robot movement, or offline, by the actuation of the redundant motor before the robot movement. The later alternative has been exploited in this manuscript. The inclusion of redundant actuators promotes the reduction of the maximum required torque to perform a predefined trajectory. For the chosen trajectory and manipulator, a 30% reduction has been verified. This results corroborates to the idea that kinematic redundancy can enhance the dynamic performance of a manipulator.

5. ACKNOWLEDGEMENTS

João C. Santos, Douglas M. Rocha and Maíra M. da Silva are thankful for their grants PIBIC/CNPq, FAPESP 2011/15605-0 and CNPq 02588/2011-6, respectively.

6. REFERENCES

Bonev, I. A., Gosselin, C. M., 2001, "Singularity Loci of Planar Parallel Manipulators with Revolute Joints", 2nd Workshop on Computational Kinematics, Seoul, South Korea, pp. 291-299.

Conkur, E.S., Buckingham, R., 1997, "Clarifying the definition of redundancy as used in robotics", Robotica Vol. 15, pp. 583 – 586.

Gosselin, C., Angeles, J., 1990, "Singularity Analysis of Closed-Loop Kinematic Chains", IEEE Transactions on Robotic and Automation, Vol. 6, No. 3, 281-290, June 1990.

Mohamed, M.G., Gosselin, C.M., 2005, "Design and Analysis of Kinematically Redundant Parallel Manipulators with Configurable Platforms", IEEE Transactions on robotics Vol. 21, No. 3, pp. 277-287.

Kotlarski, J., Abdellatif, H., Ortmaier, T., Heimann, B., 2009, "Enlarging the useable workspace of planar parallel robots using mechanisms of variable geometry". In Proc. of the ASME/IFToMM International Conference on Reconfigurable Mechanisms and Robots, London, United Kingdom, June 2009, pp. 94–103.

Kotlarski, J., Heimann, B., Ortmaier, T., 2011, "Experimental Validation of the Influence of Kinematic Redundancy on the Pose Accuracy of Parallel Kinematic Machines", IEEE International Conference on Robotics and Automation Shanghai International Conference Center, May 9-13, 2011, Shanghai, China.

Mabie H.H., Reinholtz, C.F., Mechanisms and Dynamic of Machinery, 4th edition, Wiley, 1987.

Merlet, J-P, 1996, "Redundant parallel manipulators", Laboratory Robotics and Automation, Vol. 8, No. 1, pp. 17-24.

Rao, S.S., 2009, "Engineering Optimization: Theory and Practice", Fourth Edition, John Wiley & Sons, Inc.

Rocha, D.M, da Silva, M.M., 2013, "Workspace and singularity analysis of redundantly actuated planar parallel kinematic machines", In Proc. of the XV International Symposium on Dynamic Problems of Mechanics, Búzios, RJ, Brazil, February 17-22, 2013, pp 1-10.

Siciliano, B., Khatib O., Handbook of Robotics, Springer, 2008.

Wu, J., Wang, J., You Z., A, 2011, "A comparison study on the dynamics of planar 3-DOF 4-RRR, 3-RRR and 2-RRR parallel manipulators", Robotics and Computer-Integrated Manufacturing, Vol. 27, pp. 150-156.

7. RESPONSIBILITY NOTICE

The authors are the only responsible for the printed material included in this paper.